$CeCu_2Si_2$ AND UBe_{13}: NEW QUESTIONS—OLD ANSWERS?

F. STEGLICH†[a,*], C. GEIBEL[a], R. HELFRICH[a], F. KROMER[a], M. LANG[a], G. SPARN[a], P. GEGENWART[b], L. DONNEVERT[b], C. LANGHAMMER[b], A. LINK[b], J. S. KIM[c] and G. R. STEWART‡[c]

[a]Max–Planck-Institut für Chemische Physik fester Stoffe, D-01187 Dresden, Germany
[b]Institut für Festkörperphysik, TU Darmstadt, D-64289 Darmstadt, Germany
[c]Department of Physics, University of Florida, Gainesville, FL 32611, USA

Abstract—Non-Fermi-liquid (NFL) temperature dependences of both the resistivity $\rho(T)$ and the Sommerfeld coefficient $\gamma(T)$ are observed for normal-state $CeCu_2Si_2$ and UBe_{13}. For the former compound, the NFL effects are related to the suppression (via pressure or suitable composition) of the spin-density-wave (SDW)-type 'phase A' ($T_A \rightarrow 0$). Upon approaching the quantum critical point, $\rho(T)$ and $\gamma(T)$ behave very disparately, indicating a decoupling of the itinerant and local 4*f* parts of the heavy-fermion quasiparticles. Similar observations are made with UBe_{13} for which, however, no magnetic phase transition could so far be established. New anomalies are discovered in superconducting $U_{1-x}Th_xBe_{13}$ with $0 \leq x < x_{cr} = 0.019$.

1. INTRODUCTION

The tetragonal compound $CeCu_2Si_2$ was the first of a—by now—long list of 'novel' (i.e. non-BCS) superconductors [1]. It belongs to the 'heavy-fermion' (HF) metals, in which quasiparticles composed of both local *f* degrees of freedom and itinerant conduction–electron degrees of freedom form well below the characteristic 'Kondo temperature', T_K ($\approx$15 K). The *f* degrees of freedom determine the huge effective quasiparticle mass, m^* ($\approx 300\ m_{el}$), as inferred from a giant Sommerfeld coefficient $\gamma \approx 0.7\ J\,K^{-2}\,mol^{-1}$ [1]. Both the discontinuity in the specific heat, ΔC [1], and the slope of the upper-critical-field curve, $B'_{C2} = -(dB_{C2}/dT)$ [2], at $T_C \approx 0.65$ K were found to scale with the large γ value and ascribed to massive Cooper pairs. Very similar observations were subsequently made [3] for the cubic HF metal UBe_{13} ($T_C \approx 0.9$ K). Compared with their later-discovered counterparts, UPt_3 [4], URu_2Si_2 (W. Schlabitz, J. Baumann, B. Pollit, U. Rauchschwalbe, H. M. Mayer, U. Alheim and C. D. Bredl, unpublished data, 1984 [5]), UNi_2Al_3 [6] and UPd_2Al_3 [7], $CeCu_2Si_2$ and UBe_{13} are phenomenologically more complex and less understood. On the one hand, in the first four compounds, HF superconductivity forms at T_C (0.5–2 K) out of a heavy Landau Fermi-liquid (FL) state, which coexists with antiferromagnetic (afm) order at $T < T_N$. Below T_C ($\ll T_N$), HF superconductivity and afm order coexist on a microscopic scale. On the other hand, for $CeCu_2Si_2$ an as yet unidentified (presumably SDW) 'phase A' is almost degenerate with HF superconductivity, whereas for UBe_{13} no clear-cut evidence for any kind of magnetic order exists so far. Further on, the low-temperature normal (n) states of these two 'heaviest' superconductors are characterized by strong violations of Landau FL behavior. It is the main purpose of this paper to explore the 'non-Fermi-liquid' (NFL) properties of n-state $CeCu_2Si_2$ and UBe_{13}. In addition, we report the discovery of new anomalies in the superconducting (sc) state of pure UBe_{13} and its thoriated variant, for which a very complex sc phase diagram has been established [8, 9].

*Corresponding author. Tel: +49 6151 16 2184; fax: +49 6151 16 5537; e-mail: fsteglich@techn.physik.th-darmstadt.de
†Also at Darmstadt Technical University.
‡Also at Augsburg University.

2. $CeCu_2Si_2$: BREAKDOWN OF THE HEAVY-FERMION PICTURE IN THE VICINITY OF THE A-PHASE TRANSITION

A thorough investigation of $CeCu_2Si_2$ single crystals revealed the existence of distinctly different groundstate properties, depending on the composition of the starting melt and/or the subsequent heat treatment [10, 11]. However, any differences in the lattice parameters of these different variants are much too small to be resolved by X-ray diffractometry. A subsequent systematic study of polycrystalline samples enabled Geibel *et al*. [12] to map the different physical groundstate behaviors ('S', 'AS', 'A' and 'X') to different sectors within the narrow homogeneity range of $CeCu_2Si_2$ in the chemical Ce-Cu-Si phase diagram. Phase A can be stabilized by partial Ge-substitution for Si [13]: 'A-type' $CeCu_2(Si_{1-x}Ge_x)_2$ samples, with $0 \leq x \leq 0.15$, exhibit an A-phase transition at T_A (between 0.75 K and 1.5 K), followed by an sc transition at T_C (between 0.45 K and 0.15 K). A

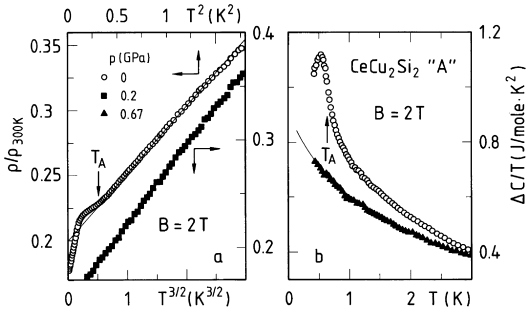

Fig. 1. (a) Resistivity, normalized to its value at $T = 300$ K, as $\rho/\rho_{300\,\mathrm{K}}$ *versus* T^2 (upper scale) and $\rho/\rho_{300\,\mathrm{K}}$ *versus* $T^{3/2}$ (lower scale); (b) as well as Ce increment to the specific heat as $\Delta C/T$ *versus* T, for $B = 2$ T and at $p = 0$, as well as 'overcritical' pressures for an 'A-type' $CeCu_2Si_2$ polycrystal. Solid line in (b) displays a fit of the SCR theory [16], implying $y_0 = 0, y_1 = 4$ and $T_0 = 13$ K, to the data.

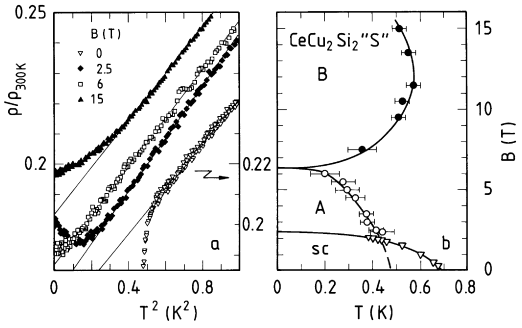

Fig. 2. (a) $\rho/\rho_{300\,\mathrm{K}}$ *versus* T^2 at $B = 0$ and differing magnetic fields for an 'S-type' $CeCu_2Si_2$ polycrystal; (b) resistively determined B–T phase diagram for the same sample indicating non-overlapping existence ranges of superconductivity, phase A and phase B. Dashed line indicates fictitious $T_A(B)$ dependence at low fields, if superconductivity were absent.

thermodynamically weak HF-sc state and phase A coexist on a microscopic scale in these 'A-type' samples [13]. In 'AS-type' $CeCu_2Si_2$ samples, showing a near stoichiometric composition and $T_A \gtrsim T_C$, HF superconductivity expels phase A below T_C [11]. Bulk measurements on 'S-type' polycrystals, prepared by using a slight Cu or Ce excess, reveal A-phase signatures only at magnetic fields sufficient to suppress superconductivity, while $B = 0$ μSR indicates the presence of a 'magnetic minority domain' whose volume fraction continuously shrinks upon cooling to well below T_C [14]. 'S-type' single crystals do not show any A-phase signatures. For all $CeCu_2Si_2$ samples of 'A-', 'AS-' and 'S-type' studied so far, an additional 'phase B' [11], phenomenologically related to phase A, was observed to form at fields $B > 6$ T§.

In the following, we shall focus on samples from the 'S sector' where the signatures for phase A are lost and NFL effects are expected [15, 16] to show up in n-state properties. To this purpose, we will discuss (i) a pressure-induced A–S transition (Fig. 1) as well as resistivity results on (ii) an 'S-type' polycrystal (Fig. 2), (iii) an 'S-type' single crystal (Fig. 3), and (iv) specific-heat results on the latter (Fig. 4).

The A-phase transition manifests itself in the $p = 0$ data of Fig. 1(a,b), taken in an overcritical field $B = 2$ T, through broadened anomalies in the T-dependences of $\rho(T)$ and $\gamma(T) = \Delta C(T)/T$, where ΔC denotes the difference in the specific heats of $CeCu_2Si_2$ and $LaCu_2Si_2$. Application of hydrostatic pressure $p > p_{cr} \approx 0.1$ GPa suffices to replace, at $B = 0$, phase A by a (thermodynamically strong) HF-sc state below $T_C = 0.65$ K. In Fig. 1, we show n-state data for $p > p_{cr}$ taken at $B = 2$ T and for $T \geq 0.4$ K. Both $\rho(T)$ and $\gamma(T)$ are found to fulfill the asymptotic behavior theoretically predicted for a three-dimensional 'nearly afm FL': $\rho = \rho_0 + \beta T^{3/2}$ [15, 16] and $\gamma = \gamma_0 - \alpha T^{1/2}$ [16]. An extension of these experiments to lower temperatures utilizing pressure cells is in preparation in order to determine the true asymptotic properties. However, from the existing results (at $p > p_{cr}$, $T \geq 0.4$ K, $B = 2$ T) we may conclude that $T_A \rightarrow 0$ indeed defines a quantum critical point (QCP) of afm nature [15, 16].

We now return to the ambient-pressure results in Fig. 1(a,b), which display a strikingly dual behavior for $T > T_A$: While $\rho = \rho_0 + aT^2$, with a giant coefficient $a \approx 10\ \mu\Omega\ \mathrm{cm}^{-1}\ \mathrm{K}^{-2}$, seems to indicate that the A-phase transition occurs out of a heavy Landau FL state, the strongly T-dependent, $\gamma(T)$, is not compatible with such an interpretation. Quite generally, we have observed that in $CeCu_2Si_2$, $\Delta\rho = \rho - \rho_0 = aT^2$ is always preceding an A- or B-phase transition. This is shown for the S-type polycrystal in the whole field range $0 \leq B \leq 15$ T [Fig. 2(a)] as well as for the S-type single crystal at fields $B > 6$ T (Fig. 3). As indicated in Fig. 3(b), the limiting temperature T_L for this T^2 dependence is tracking the magnetic-field dependence of the corresponding

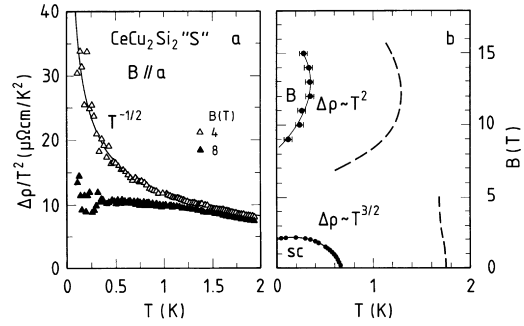

Fig. 3. (a) Resistivity as $\Delta\rho/T^2$ *versus* $T(\Delta\rho = \rho - \rho_0)$ at $B = 4$ T and 8 T for an 'S-type' $CeCu_2Si_2$ single crystal. Solid line indicates $T^{3/2}$ dependence of $\Delta\rho(T)$; (b) resistively determined B–T phase diagram for the same crystal, indicating existence ranges of superconductivity and phase B. Dashed lines mark limiting temperatures for $T^{3/2}$ and T^2 dependences of $\Delta\rho(T)$, respectively.

§For 'X-type' $CeCu_2Si_2$, static afm order with small moment ($\mu_S \approx 0.01\mu_B$) was recently established via Cu-NQR (Y. Kitaoka, private communication, 1997).

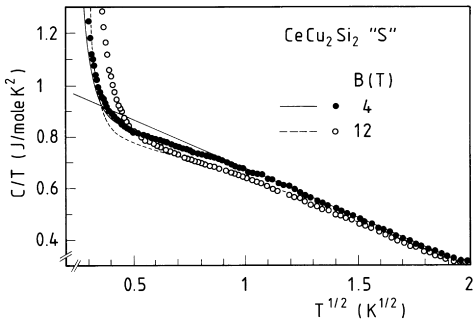

Fig. 4. $\gamma = C/T$ *versus* $T^{1/2}$ at $B = 4$ T and 12 T for the same crystal as in Fig. 3. Straight solid line indicates $(-T^{1/2})$ dependence of $\gamma(T) - \gamma_0$. The other lines indicate $C(T)/T$ data after subtraction of nuclear hyperfine contributions due to the applied B fields.

phase-transition temperature. We have recently observed that this also holds true for the dependences of T_L and T_A on (subcritical) pressure [17]. From these findings, one might be inclined to ascribe the $\Delta\rho = aT^2$ dependence to some critical fluctuations precursive to the A/B transition. However, a linear T dependence of $\Delta\rho(T)$ is expected, preceding an itinerant afm phase transition [18].

Note that in the case of the 'S-type' polycrystal, where phase A exists at overcritical fields and is expelled to a large extent [14] by HF superconductivity at low fields, the n-state resistivity follows a T^2 dependence (Fig. 2(a)). In the case of the 'S-type' single crystal, however, which does not exhibit any A-phase signatures, the low-T resistivity at $B < 6$ T is well described by $\Delta\rho = \beta T^{3/2}$ (Fig. 3). At elevated temperatures ($T > 0.6$ K), this goes along with $\gamma = \gamma_0 - \alpha T^{1/2}$ (cf. $B = 4$ T data in Fig. 4). As with the polycrystal data of Fig. 1, taken at overcritical pressures, we infer from these ambient-pressure results on the single crystal, the existence of an afm QCP, associated with the vanishing of the A-phase transition temperature.

Below, we wish to compare the resistivity and specific-heat results taken on this same single crystal at lower temperatures and/or at higher B fields. These results clearly show that upon approaching the QCP, $\Delta\rho(T)$ (probing the itinerant part of the heavy fermions) and $\gamma(T)$ (determined by the local 4*f* degrees of freedom) behave, qualitatively, very differently from each other. We first notice that the gross change from $\Delta\rho \sim T^{3/2}$ to $\Delta\rho \sim T^2$ when B is raised to $B > 6$ T (Fig. 3), has no correspondence in the $\gamma(T)$ results (Fig. 4). Next, we compare the $B = 4$ T data for $\Delta\rho(T)$ with those for $\gamma(T)$. As shown in Fig. 3(a), $\Delta\rho(T)/T^2$ which measures the cross section for quasiparticle–quasiparticle scattering keeps rising proportional to $T^{-1/2}$ down to the lowest temperatures. However, $\Delta\gamma = \gamma - \gamma_0$ does *not* follow the corresponding $(-T^{1/2})$ dependence (straight line in Fig. 4).

The $T^{-1/2}$ divergence of the quasiparticle–quasiparticle cross section indicates singular scattering mediated by extremely soft (and spatially extended) afm fluctuations at the QCP [15, 16]. However, since the latter are restricted to wave vectors in the vicinity of the afm ordering wave vector, $\mathbf{Q}_{afm}$, quasiparticle states at certain lines on the Fermi surface only ought to undergo this singular scattering. Following [19], the ordinary quasiparticle–quasiparticle scattering events of all other states on the Fermi surface result in the usual law $\Delta\rho = aT^2$, which must short-circuit the anomalous $\Delta\rho = \beta T^{3/2}$ term at sufficiently low temperatures. We cannot resolve such a crossover in our data taken at $B < 6$ T down to $T = 20$ mK. Interestingly enough, below $T = 0.6$ K the T-dependence of $\gamma(T)$ flattens somewhat (Fig. 4), as if a Landau FL state were approached as $T \to 0$. A detailed analysis is, however, prevented by a steep upturn in $\gamma(T)$ below $T = 0.25$ K. The latter cannot be attributed to the Zeeman splitting of the nuclear Cu/Si spin states by the external B-field, cf. the other (solid and dashed) lines in Fig. 4.

In summary, when approaching the A-phase transition, both at $T_A > 0$ and $T_A \to 0$, we are unable to describe our resistivity and specific-heat results in any consistent way. This strongly suggests a breakdown of the concept of heavy quasiparticles. Rather, near the A-phase transition, their itinerant conduction-electron and local 4*f* components appear decoupled from each other.

3. UBe_{13}: NON-FERMI-LIQUID NORMAL STATE AND NEW ANOMALIES BELOW T_c

Two variants of UBe_{13} with markedly different sc and n-state properties have recently been identified [20]: 'H-type' ($T_C \approx 0.9$ K) and 'L-type' ($T_C \approx 0.75$ K) UBe_{13}. Since the former variant is mostly found among polycrystals while all 'L-type' samples are single crystals, we believe that their phenomenological differences must be related to differences in the actual composition originating in different preparation procedures [20].

In the following, we discuss some low-T properties of a high-quality UBe_{13} single crystal of 'H type'. At $T \approx 2$ K, the electrical resistivity assumes its maximum value, indicating an inelastic mean free path as short as a few lattice spacings. Usually some, as yet unidentified, afm spin fluctuations are blamed for the high n-state resistivity. As indicated in Fig. 5, these '2 K fluctuations' seem to be efficiently suppressed already by moderate magnetic fields: in a wide field range, $4\text{ T} \leq B \leq 10$ T, we find $\rho(T)$, normalized to the respective value at $T = 1$ K, to behave in a universal way, i.e. $\rho \sim T$ around $T = 1$ K and $\rho = \rho_0 + \beta T^{3/2}$ below $T \approx 0.8$ K [Fig. 5(b) and Fig. 6(a)]. This NFL behavior is in accord with the prediction for the three-dimensional 'nearly afm FL' [16]. For the highest B-fields of 14 T and 15.5 T and below $T \approx 0.3$ K, a

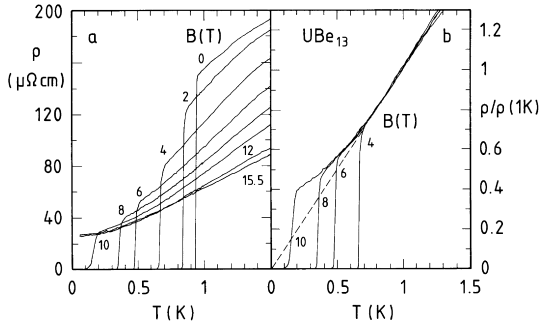

Fig. 5. (a) ρ *versus* T for an 'H-type' UBe_{13} single crystal at $B = 0$ and differing magnetic fields; (b) same data as in (a), normalized to the respective ρ value at $T = 1$ K. Dashed line is an extrapolation to $T = 0$ of the data for $T \geq 0.8$ K.

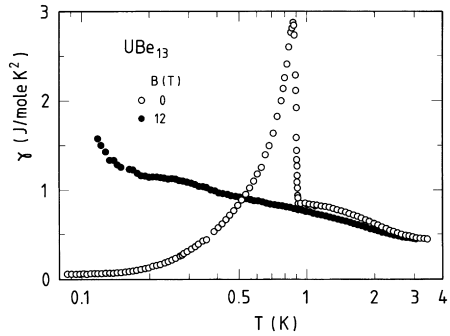

Fig. 7. $\gamma = C^*/T$ *versus* T (on a logarithmic scale) at $B = 0$ and 12 T for the same crystal as in Fig. 5. $C^* = C - C_N$, C_N: nuclear hyperfine contribution due to the external B field.

deviation from the $T^{3/2}$ law is noticed. As demonstrated in the inset of Fig. 6(b), these low-T data can be well fit by $\Delta\rho = aT^2$. The gigantic coefficient a is found to decrease with increasing field, i.e. from 52 $\mu\Omega$ cm K^{-2} at $B = 14$ T to 45 $\mu\Omega$ cm K^{-2} at $B = 15.5$ T. At present, it is not clear whether this asymptotic T^2 term also exists at low field, where it is masked by the sc transition, or whether it is induced by the high magnetic field. We recall that already at low field, a crossover from $T^{3/2}$ to T^2 at a sufficiently low temperature must necessarily occur [19] for a 'nearly afm FL'. However, this is unlikely to be realized in UBe_{13}: The isothermal n-state magnetoresistance, $\Delta\rho(B)$, is found to be negative below $T = 2$ K in the whole field range, $B < 14$ T. A negative sign of $\Delta\rho(B)$ is typical for a NFL [21], while a positive one is a hallmark of the Landau FL. In fact, for $B \geq 14$ T $\Delta\rho(B)$ becomes positive at the same low temperatures where $\Delta\rho(T)$ follows the T^2 law, cf. inset of Fig. 6(b).

The specific-heat coefficient $\gamma(T) = C^*(T)/T$ is shown for the same UBe_{13} single crystal in Fig. 7. Here, $C^*(T) = C(T) - C_N(T)$ where $C_N(T)$ is the nuclear hyperfine contribution, calculated for the externally applied field. At $B = 12$ T, $\gamma(T)$ increases approximately logarithmically upon cooling to $T \approx 0.3$ K. Very similar to our observations with the S-type $CeCu_2Si_2$ single crystal (Fig. 4), $\gamma(T)$ of n-state UBe_{13} tends to flatten at intermediate temperatures, before it starts to steeply increase at the low-T end. To summarize, our findings for n-state UBe_{13} resemble the ones made for $CeCu_2Si_2$ near its QCP, though there is no clear-cut evidence for afm order in the former compound. A more careful analysis of the NFL n-state of UBe_{13} is, however, hampered by the large value of its upper critical field.

In the remainder of this section, we wish to focus on the HF-sc state of UBe_{13}. Fig. 8 displays some of the phenomenological differences between 'H-type' and 'L-type' UBe_{13} samples. For example, the positive anomaly in the T dependence of the n-state thermal expansion, $\alpha(T)$, is shifted from $T \approx 2$ K ('H type'), to $T \approx 1.2$ K ('L type'), cf. Fig. 8(a). This anomaly was ascribed [22] to local Kondo-type spin fluctuations. Further on, $B_{C2}(T)$ being extremely steep near T_C shows an increase in slope near $T_C/2$ for 'H-type' UBe_{13}, which is absent for the 'L-type' sample [Fig. 8(b)]. Also shown in Fig. 8(b) is a new 'line of anomalies', $B^*(T)$, established for 'H-type' UBe_{13}, both in isothermal field scans of the specific heat [22] and in $\alpha(T)$ measured at zero field [Fig. 8(a)]

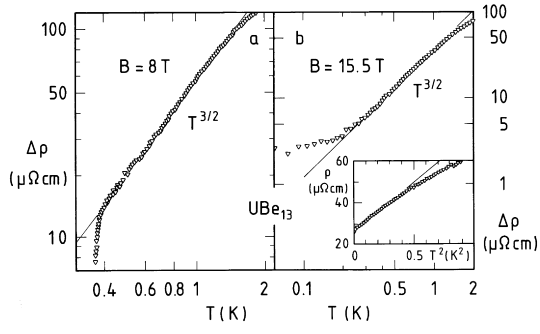

Fig. 6. Double-log plot of $\Delta\rho = \rho - \rho_0$ *versus* T for the same crystal as in Fig. 5 at (a) $B = 8$ T and (b) $B = 15.5$ T. Inset shows low-T data of (b) as ρ *versus* T^2.

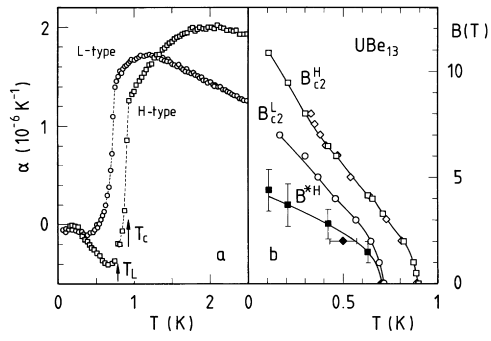

Fig. 8. (a) Coefficient of the linear thermal expansion measured along [100], α *versus* T, for the same 'H-type' UBe_{13} single crystal as in Fig. 5 and for an 'L-type' single crystal. Arrows mark for the 'H-type' crystal superconducting transition temperature, T_C and temperature of the broadened lower transition, T_L, see text; (b) upper critical field curves, $B_{C2}(T)$, for the same crystals as in (a) (open symbols) and new 'line of anomalies', $B^*(T)$, starting at $T = T_L(B = 0)$, for the 'H-type' crystal (full symbols) as determined by $\alpha(T, B = \text{const.})$ (◇, ○, ◆) and $C(B, T = \text{const.})$ (□, ■), respectively.

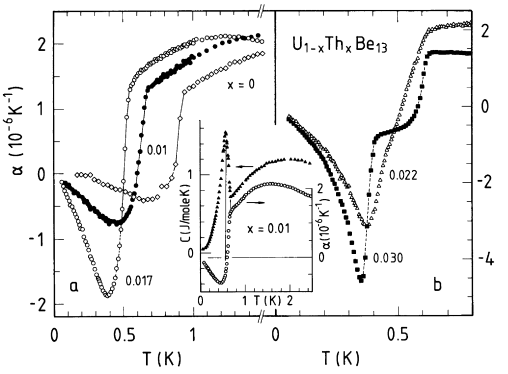

Fig. 9. (a) Coefficient of the linear thermal expansion as α *versus* T for the same 'H-type' UBe_{13} single crystal as in Fig. 5 and for polycrystalline $U_{1-x}Th_xBe_{13}$ samples with $x = 0.01$ and 0.017 ($<x_{cr}$); (b) as well as $x = 0.022$ and 0.03 ($>x_{cr}$). Inset shows $C(T)$ and $\alpha(T)$ for $x = 0.01$ sample. Vertical lines indicate the width of superconducting transition in $C(T)$, used to separate the corresponding anomaly from the $\alpha(T)$ data.

or at constant, finite fields. Note that the negative and distinctly asymmetric thermal-expansion anomaly which occurs below T_C is almost completely suppressed by a field $B = 4$ T which is, however, not sufficient to suppress the large sc jump anomaly [22].

As is seen in Fig. 9(a), this $\alpha(T)$ minimum sharpens and shifts toward lower temperatures upon doping with Th. In the inset we show for the $x = 0.01$ sample how, with the help of the specific-heat results, the sc jump anomaly can be separated from the $\alpha(T)$ data, leaving behind the broad $\alpha(T)$ minimum. The (steeper) high-temperature part of this broad anomaly is then replaced in an 'equal-areas construction' by an idealized sharp jump. This defines the 'position of the anomaly', i.e. T_L at $B = 0$. Comparison of the data for $x = 0.017$ [Fig. 9(a)] with those for $x > 0.019$ [Fig. 9(b)] strongly suggests that the lower phase-transition anomaly for $U_{1-x}Th_xBe_{13}$ samples with 'critical' Th concentrations [8, 9] evolves out of the negative $\alpha(T)$

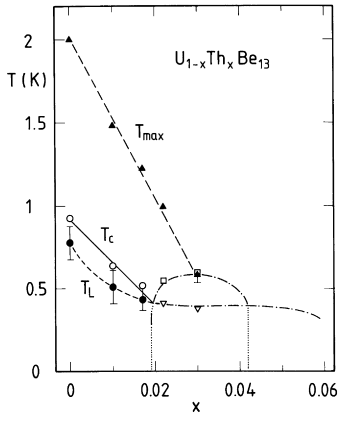

Fig. 10. T–x phase diagram of $U_{1-x}Th_xBe_{13}$ including results from the literature (— · —[9]; ·· - ··[23]) and the present study: open symbols indicate second-order phase transitions, while closed symbols mark anomalies at $T_L(x)$ (●) and $T_{max}(x)$ (▲), as described in the text.

anomaly, as established in the subcritical concentration range. In addition, at $x_{cr} = 0.019$ the 'line of anomalies' denoted by $T_L(x)$ in the T–x phase diagram of Fig. 10 seems to merge smoothly into the $T_{C2}(x)$ line, indicating the lower of the two second-order phase transitions [8, 9]. No doubt, our observations pose serious constraints to any theoretical model attempting to explain HF superconductivity in pure UBe_{13} and its thoriated derivative (see e.g. [24]).

Finally, we wish to comment on the line denoted $T_{max}(x)$ which hits the upper phase transition line, $T_{C1}(x)$, almost at its maximum value. $T_{max}(x)$ indicates the position of a Kondo-type $\alpha(T)$ anomaly in the n-state, cf. Fig. 8(a). In [22] an effective two-band model for $U_{1-x}Th_xBe_{13}$ was proposed. In this model, HF superconductivity is carried by 'less localized 5*f* states' (with $T_{K1} = 10$–30 K). The latter are scattered by the Kondo fluctuations of the 'more localized 5*f* states' ($T_{K2} \approx T_{max}$): Once $T_{max}(x)$ becomes smaller than $T_{C1}(x)$, an additional pair-breaking channel opens and destabilizes superconductivity [22].

4. CONCLUSIONS

HF superconductivity in $CeCu_2Si_2$ as well as in UBe_{13} forms out of a NFL normal state. For $CeCu_2Si_2$, anomalous T-dependences at intermediate temperatures ($T > 0.6$ K) and sufficiently low magnetic fields ($B < 6$ T) are strongly suggesting an afm QCP on the brink of phase A ($T_A \rightarrow 0$). When approaching this QCP by further cooling, however, $\Delta\rho(T)$ and $\gamma(T)$ behave quite disparately. This highlights a decoupling of the itinerant and local (4*f*) parts of the heavy-fermion quasiparticles. But even when T_A is finite, $\Delta\rho(T)$ and $\gamma(T)$ behave strikingly differently upon approaching the A-phase transition. Above the QCP, $\Delta\rho(T)$ is proportional to $T^{3/2}$ down to mK temperatures. The absence of a low-T crossover to $\Delta\rho \approx T^2$ is hard to understand on the basis of a 'nearly afm FL' [19].

For UBe_{13}, the incoherent normal state is caused only to a smaller part by the so-called '2 K fluctuations'. When these are suppressed by a moderate magnetic field, a universal T-dependence of the n-state resistivity is recovered in a wide range of magnetic fields. $\Delta\rho(T)$ indicates NFL properties compatible with an afm QCP, too, but so far no convincing evidence for afm order has been found in this compound. Though a detailed analysis of the n-state properties is impeded by the unusually high B_{C2} values, similar inconsistencies concerning the 'nearly afm FL scenario', as stated above for $CeCu_2Si_2$, seem to exist for UBe_{13} as well. New anomalies in the sc state of both UBe_{13} and $U_{1-x}Th_xBe_{13}$ with subcritical Th concentrations are identified as precursors of the lower phase transition, previously established [8, 9] in the critical concentration range $0.019 < x < 0.045$.

Acknowledgements—We are grateful to W. Assmus for supplying the $CeCu_2Si_2$ single crystal. We acknowledge a fruitful correspondence with P. Coleman. Work in Darmstadt was supported by the SFB 252, work in Gainesville by the US Department of Energy, Contract no. De-FG05-86ER45258.

REFERENCES

1. Steglich, F., Aarts, J., Bredl, C. D., Lieke, W., Meschede, D., Franz, W. and Schäfer, H., *Phys. Rev. Lett.*, 1979, **43**, 1892.
2. Rauchschwalbe, U., Lieke, W., Bredl, C. D., Steglich, F., Aarts, J., Martini, K. M. and Mota, A. C., *Phys. Rev. Lett.*, 1982, **49**, 1448.
3. Ott, H. R., Rudigier, H., Fisk, Z. and Smith, J. L., *Phys. Rev. Lett.*, 1983, **50**, 1595.
4. Stewart, G. R., Fisk, Z., Willis, J. O. and Smith, J. L., *Phys. Rev. Lett.*, 1984, **52**, 679.
5. Schlabitz, W., Baumann, J., Pollit, B., Rauchschwalbe, U., Mayer, H. M., Ahlheim, U. and Bredl, C. D., *Z. Phys. B*, 1986, **62**, 171.
6. Geibel, C., Thies, S., Kaczorowski, D., Mehner, A., Grauel, A., Seidel, B., Ahlheim, U., Helfrich, R., Petersen, K., Bredl, C. D. and Steglich, F., *Z. Phys. B*, 1991, **83**, 305.
7. Geibel, C., Schank, C., Thies, S., Kitazawa, H., Bredl, C. D., Böhm, A., Rau, M., Grauel, A., Caspary, R., Helfrich, R., Ahlheim, U., Weber, G. and Steglich, F., *Z. Phys. B*, 1991, **84**, 1.
8. Ott, H. R., Rudigier, H., Fisk, Z. and Smith, J. L., *Phys. Rev. B*, 1985, **31**, 1651.
9. Heffner, R. H., Smith, J. L., Willis, J. O., Birrer, P., Baines, C., Gygax, F. N., Hitti, B., Lippelt, E., Ott, H. R., Schenck, A., Knetsch, E. A., Mydosh, J. A. and MacLaughlin, D. E., *Phys. Rev. Lett.*, 1990, **65**, 2816.
10. Lang, M., Modler, R., Ahlheim, U., Helfrich, R., Reinders, P. H. P., Steglich, F., Assmus, W., Sun, W., Bruls, G., Weber, D. and Lüthi, B., *Physica Scripta T*, 1991, **39**, 135.
11. Bruls, G., Wolf, B., Finsterbusch, D., Thalmeier, P., Kouroudis, I., Sun, W., Assmus, W., Lüthi, B., Lang, M., Gloos, K., Steglich, F. and Modler, R., *Phys. Rev. Lett.*, 1994, **72**, 1754.
12. Steglich, F., Gegenwart, P., Geibel, C., Helfrich, R., Hellmann, P., Lang, M., Link, A., Modler, R., Sparn, G., Büttgen, N. and Loidl, A., *Physica B*, 1996, **223/224**, 1.
13. Geibel, C., *Phys. B1*, 1997, **53**, 689.
14. Feyerherm, R., Amato, A., Geibel, C., Gygax, F. N., Hellmann, P., Heffner, R. H., MacLaughlin, D. E., Müller-Reisener, R., Niewenhuys, G. J., Schenck, A. and Steglich, F., *Physica B*, 1995, **206/207**, 596.
15. Millis, A. J., *Phys. Rev. B*, 1993, **48**, 7183.
16. Moriya, T. and Takimoto, T., *J. Phys. Soc. Jpn.*, 1995, **64**, 960.
17. Sparn, G., Donnevert, L., Hellmann, P., Laube, F., Link, A., Thomas, S., Gegenwart, P., Buschinger, B., Geibel, C. and Steglich, F., *Rev. High Pressure Technol.*, 1998, **7**, 431.
18. Ueda, K., *J. Phys. Soc. Jpn.*, 1977, **43**, 1497.
19. Hlubina, R. and Rice, T. M., *Phys. Rev. B*, 1995, **51**, 9253.
20. Langhammer, C., Helfrich, R., Bach, A., Kromer, F., Lang, M., Michels, T., Deppe, M., Steglich, F. and Stewart, G. R., *J. Magn. Magn. Mat.*, 1998, **177–181**, 443.
21. Steglich, F., Gegenwart, P., Helfrich, R., Langhammer, C., Hellmann, P., Donnevert, L., Geibel, C., Lang, M., Sparn, G., Assmus, W., Stewart, G. R. and Ochiai, A., *Z. Phys. B*, 1997, **103**, 235.
22. Kromer, F., Helfrich, R., Lang, M., Steglich, F., Langhammer, C., Bach, A., Michels, T., Kim, J. S. and Stewart, G. R., *Chin. J. Phys. (Taipei)*, 1998, **36**, 157.
23. Zieve, R. J., Jin, D. S., Rosenbaum, T. F., Kim, J. S. and Stewart, G. R., *Phys. Rev. Lett.*, 1994, **72**, 756.
24. Sigrist, M. and Rice, T. M., *Phys. Rev. B*, 1989, **39**, 2200.